VOL. 7, NO. 5, MAY 2012 ISSN 1819-6608
ARPN Journal of Engineering and Applied Sciences


www.arpnjournals.com

ULTRASONIC CHARACTERIZATION OF FREQUENCY-DEPENDENT ATTENUATION IN PLASTER BOARDS

Asafa Tesleem B.
Department of Mechanical Engineering, King Fahd University of Petroleum and Minerals, Dhahran, Saudi Arabia
E-Mail: g200902430@kfupm.edu.sa

ABSTRACT

Plaster boards are heterogeneous materials with substantial degree of attenuation when ultrasonic waves pass through them. The attenuation properties are determined from the frequency shifts induced by the presence of scatterers within the material continuum. In this work, I used the principle of ultrasonic to estimate the frequency shifts in three different plaster boards which are: Cement Board (CB), Glass Fiber Reinforced Gypsum (GRG) and Exterior Glass fiber Reinforced Gypsum (EGRG). Few samples were obtained from these boards and each sample was partitioned into 49 grids from where signals were extracted with Harisonic 2.25MHz transducer operated in a contact mode. The signals were processed using time domain and homomorphic analyses. Histograms of the time domain analysis indicate a general shift towards low amplitudes with conspicuous non-uniformity in the shift magnitude. The skewness and standard deviation of the frequency shifts clearly show some fundamental differences in the nature of scattering and absorption in these materials. Downwards shifts in the centre frequencies compared to the steel reference material are equally significant. The mean center frequencies are found to be 2.3891, 2.2695 and 2.2102MHz for CB, GRG and EGRG respectively which indicates that CB has the lowest attenuation. Also, attenuations are found to increase with increase in frequency within the range of the transducer bandwidth (2.0286 and 3.4402 MHz). Tests of repetitions confirm that the observed frequencies changes are due to the scatterers in the samples and not signal processing artifacts.

Keywords: ultrasonics, plaster boards, homomorphic, center frequency, attenuation.

1. INTRODUCTION

Plaster boards are used for finishing and decorations of building interiors and other architectural edifices. Knowledge of their attenuation property is important for designing and selection of ultrasonic techniques for probing their microstructures [1]. Ultrasonic attenuation in metals and their subsequent characterization have received several attentions [2] while little has been done on plasterboards. Papadakis [3] and Evans *et al*., [4] were among the early researchers in ultrasonic base metal characterization. Saniie *et al*., [5], Saniie and Bilgutay [6], Fakuhara *et al*., [7], Cantrell and Yost [8] and Bouda [9] also worked extensively on ultrasonic attenuation in metals and metallic materials [10]. Few researchers also measured attenuation in cement-based materials; among them are Tasker *et al*., [11], Gaydecki *et al*., [12], Landis and Shah [13], Joseph and Laurence [14], Laurence and Joseph [10] and most recently Aggelis [2]. In spite of the large amount of materials in this area, no published article is available on gypsum-based materials.

Because of microstructural homogeneity in metals and metallic materials, attenuation is less significant and backscattered echoes are often very distinct from background noise making magnitude spectrum easily obtainable via Fast Fourier Transformation (FFT). This resulting attenuation is readily extracted from the difference of two consecutive backscattered echo spectra [2]. However, in plaster boards, backscattered echoes are hardly distinguished due to non-homogenous microstructural distribution making extraction of magnitude spectrum a very challenging task. In order to overcome this challenge, homomorphic signal processing technique is found applicable. Though, the process was used by Saniie and Bilgutay [5] for metal characterization via frequency shifts, it has however not been used for plaster boards. The process has been examined and found to be appropriate for extraction of magnitude spectrum and attenuation due to frequency shift in plaster board and by generalization in gypsum based materials.

2. THEORY OF GRAIN SIZE AND ATTENUATION MEASUREMENT

Structural materials are composed of atoms and molecules that are ideally continuum [2]. Though, design engineers assume some levels of structural continuity and homogeneity of material composition, these properties never exists in the absolute term. The homogeneity, uniformity, mechanical and structural properties of most materials are based on the individual grain size and distribution. Botvina *et al*., [16] reported that the attenuation of ultrasonic waves and mechanical properties of industrial materials and products are dominated by the same features of microstructures. It is, therefore, not surprising that the applications of ultrasonic have received a great attention in recent time. In addition to its application for detection of cracks, discontinuities, voids or inclusions that are present in metals, non-metals and composites [10], ultrasonic has also been applied for grain size determination, stress and material degradation [8, 17]. Lower cost and less time consumption of data processing compared to destructive test is another factor that is responsible for a shift towards experimental approach for establishing strong correlation between ultrasonic data and microstructural features of industrial materials.

Grain size may be determined by attenuation, scattering or ultrasonic velocity measurement. In the method of attenuation measurement, decay in ultrasonic signal amplitude obtained from reflection at back surface of material under examination is used to correlate between attenuation and material properties [5]. Typically, under a uniform test condition, the grain size is estimated by comparing the ultrasonic attenuation obtained from material of unknown grain size with specimen of known grain size. The method is however limited by the fact that parallel and flat surface is a necessary condition for the accuracy of the expected signal which is often reduced by surface irregularities. Scattering/backscattered measurement technique involves the use of grain noise signal which yields information regarding the variation in the scattered energy with respect to sample dept and hence the distribution of the grain size [18]. The method, however, requires substantial signal processing. The ultrasonic velocity technique is based on the principle of velocity-to-grain size relation as discussed elsewhere [19].

The principle of frequency attenuation may be explained by the mechanism of absorption, scattering and beam spreading [15,20,21]. Absorption is a mechanism by which wave energy is dissipated in the form of heat energy when ultrasonic energy transits across a material. Absorption may also be considered as a material effect such as viscoelastic behavior or the internal friction due to the work done at material interfaces when two materials are not elastically bonded [15]. Scattering is a phenomenon involving refraction, reflection, diffraction and mode-changing of travelling wave at discontinuities on the surface or within the medium [17]. The degree of scattering is found to be dependent on the length, density and distribution of scatterers, ultrasonic wavelength, scatterers shape (elongated, flattened, equiaxial or mixed) and random orientation of the crystals [5,16]. However, beam spreading is a geometric attenuation that includes transducer aperture diffraction, a situation where the finite dimensions of a transducer cause deviations from the ideal plane or spherical wave hypothesis.

The behaviour of ultrasonic wave in a material medium can be modeled by considering a wave of initial amplitude A_o moving through a medium in which the amplitude A of the attenuated signal at position z (corresponding to time t) are related by a decaying exponential function. Thus:

$$A = A_o \alpha_s(z,f) e^{-2\int_0^z \alpha(z,f)dz} \quad (1)$$

Where $\alpha_s(z,f)$ and $\alpha(z,f)$ are the position- and frequency-dependant scattering and attenuation coefficients respectively. If the material is considered to be homogeneous, then the attenuated amplitude becomes:

$$A = A_o \alpha_s(f) e^{-2\alpha(f)z} \quad (2)$$

Where $\alpha(f) = \alpha(z,f)$ and $\alpha_s(f) = \alpha_s(z,f)$.

The attenuation coefficient is the sum of scattering coefficient $\alpha_s(f)$ and absorption coefficient $\alpha_a(f)$ written as:

$$\alpha(f) = \alpha_s(f) = \alpha_s + \alpha_a(f) \quad (3)$$

Though, grain scattering losses are large compared to absorption losses, the later increase linearly with frequency while the former depends on the ratio of sound wavelength in the material to that of the grain diameter [3,15]. For the ultrasonic wave excited into a material in pulse-echo mode, the received signal at time τ is typically due to scatterer within the material at a distance, d, given by $d = \frac{vT}{2}$ where v is the velocity of sound propagation within the material medium. For a stationary scatterer, the amplitude of the detected signal at a fixed time after transmission of a pulse will be constant for a fixed transducer position. The measured signal within the sample can be segmented into a fixed time domain r_j corresponding to a fixed spatial interval as shown in Figure-1 as:

$$\Delta d = d_{j+1} - d_j \quad (4)$$

The measured signal is estimated from:

$$r(t) = \sum_{j=1}^{q} r_j(t) \quad (5)$$

Where r_j (t) is the signal from region j and q is the number of segmented regions. For a given region j within the sample, the backscattered echo signal can be modeled by [5]:

$$r(t) = \sum_{k=1}^{N_j} A_{kj} \{u_j(t - \tau_{kj})\}, j = 0,1,2 \ldots q \quad (6)$$

where τ_{kj} is a random variable corresponding to the random echo detection time and can be estimated from $\frac{2d_j}{v} < \tau_{kj} < \frac{2d_{j+1}}{v}$, $< u_j >$ is the mean shape of the echo (i.e., wavelet) corresponding to the jth region of the sample, A_{kj} is a random variable equivalent to average reflection coefficient of a scatterer in the region j from where echoes are detected after a delay of τ_{kj}. This depends on scattering elastic constant, cross-sectional area, ultrasonic velocity and densities of adjacent grains [5]. N_j is the number of scatterers in the region j. Taking the Fast Fourier Transformation (FFT) of the mean ultrasonic wavelet within the segmented regions, then we have a magnitude spectrum given as [13]:

$$\{U_{j+1}(w)\} = e^{-2[\alpha_j(w) - i\beta(w)]\Delta d} \{U_j(w)\} \quad (7)$$

Where $w = 2\pi f$, $\beta(w) = \frac{w}{v}$, $i = \sqrt{-1}$, $\alpha(w)$ is the attenuation coefficient due to scattering and absorption. Saniie and Bilgutay [8] pointed out that the echo $\langle U_j(w) \rangle$ could be approximated as a time limited rf-echo with a distribution similar to a Gaussian envelop

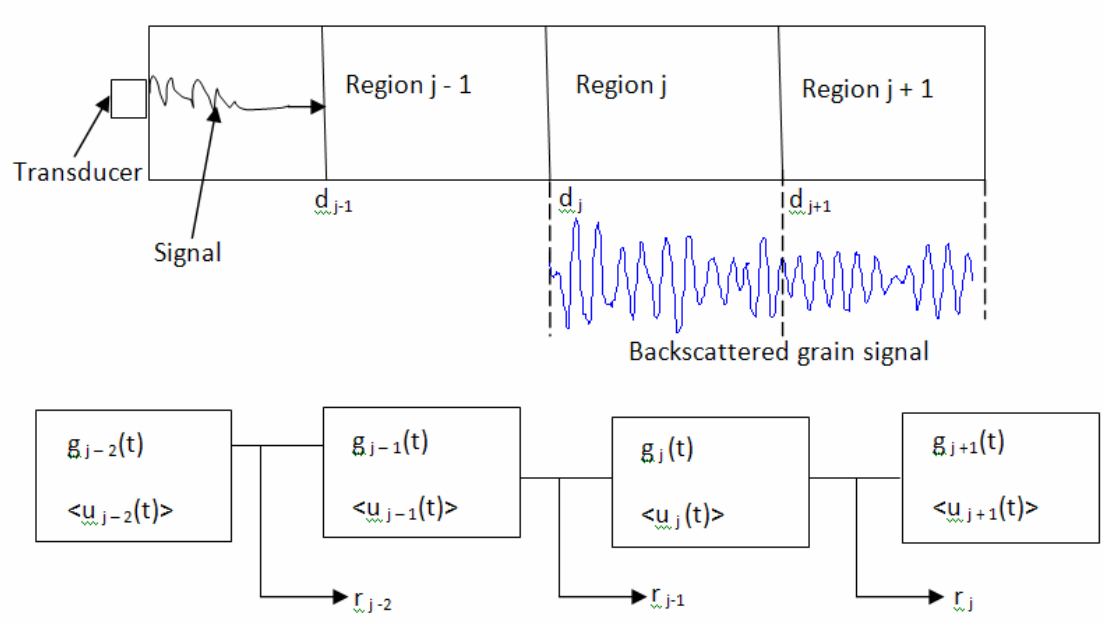

Figure-1. Signal segmentation for a sample under ultrasonic testing using backscattered echo (a) a typical backscattered grain signal corresponding to region j and j+1 (b) segmented model of backscattered signal (adapted from [5]).

given as $\langle u_j(t) \rangle = \rho_j e^{-\frac{t^2}{2\sigma_j^2}} \cos(w_j t)$. The equation is a heuristic model shedding more light into the characteristic composite of ultrasonic signal. The frequency spectrum $\langle u_j(t) \rangle$ is estimated from equation (8).

$$\langle u_j(t) \rangle = \rho_j e^{\frac{-\sigma_j^2 (w - w_j)^2}{2}} \quad (8)$$

Where conditions $w \geq 0$, $w_j \geq w_i$, $\rho_j \geq \rho_i$ and $i > j > 1$ hold and in terms of mean frequency $\langle w_j \rangle$ and for the wavelet power ρ_j , the conditions $w_j \geq w_i$, $\rho_j \geq \rho_i$ and $i > j > 1$ hold. From equations (7) and (8) and the associated conditions, the frequency-dependant attenuation coefficient is given as:

$$\alpha_j(w) = \frac{log|\langle U_j(w) \rangle| - log|\langle U_{j+1}(w) \rangle|}{2\Delta d} \quad (9)$$

It is therefore desired to find an appropriate method to evaluate the mean wavelet in order to estimate the value of attenuation due to frequency shifts. In the next section, I discussed the methodology of the signal extraction and processing.

3. EXPERIMENTAL METHOD

Three materials - CB, GRG and EGRG - with dimension 15 x 15 x 1.2cm obtained from a plaster board companies in London were used for this study. CB is a combination of cement bonded particle and glass fibers; GRG is a composition of high strength gypsum reinforced with glass fiber while EGRG is a composite of GRG and polymer. Experiments were conducted on the above samples using Harisonic CR0012 transducer of 1.905cm nominal diameter, diagnostic sonar pulser receiver model 505 5PR and LeCroy 9310 dual 300MHz oscilloscope. A steel reference material with dimension 10 x 6 x 2cm was first scanned to establish reference characteristics. The pulser receiver was optimally adjusted with the following operating conditions: repetition rate - 2, pulse energy - 1, attenuation - 50dB and damping of 4. The settings for the oscilloscope were: voltage division - 100mV, time division - 5µs and zero time delay. The relative pulse-echo sensitivity was obtained from the frequency response data by using a sinusoidal burst procedure amplified by a broadband radio frequency (rf) receiver and its A-scan image was acquired using data acquisition software available in the workstation. Signals were obtained by a direct contact between the transducer and the steel sample. To improve the acoustic matching between the transducer and the steel sample, I have used Sonotec industrial ultrasound couplant. The transducer's sensitivity was then extracted from the relationship between the amplitude of

the voltage applied to the transducer and the amplitude of the back echo. The experimental workstation is shown in Figure-2. Each sample was then divided into 49 grids where each grid measures 2cm by 2cm. The data were analyzed using time domain and homomorphic analysis techniques.

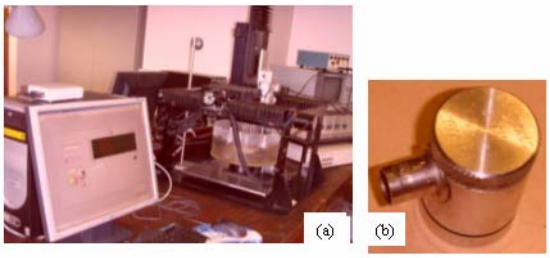

Figure-2(a). The picture of the experimental workstation **(b)** Harisonic 2.25MHz Transducer.

3.1 Time domain and homomorphic deconvolution techniques

The time domain analysis is carried out to access the degree of absorption and scattering of ultrasonic waves in the three samples. To do this, the background noise was first filtered using an optimized Gaussian signal smoothing [20]. The width of the smooth σ is related to the FWHM (full width at half maximum).

$$FWHM = \sigma * \sqrt{8\log(2)} \quad (10)$$

The FWHM was determined from the sample signals by randomly chosen data; this gave an average value of 7. Using equation (10), the σ was estimated to be 2.9726 and a smooth width of 3 was chosen. As discussed in section 2, each signal was divided into two regions (j and j+1) and histogram of the regions were plotted and superimposed in order to evaluate the shift in amplitudes and frequencies. In addition, mean, median, mode, standard deviation and skewness of each region were estimated.

The homomorphic signal processing is more complicated than the time domain analysis and most of the equations derived in section 2 are utilized. Basically, homomorphic signal processing is a branch of non-linear signal processing that utilizes Fourier transformation (FT) and logarithmic operations to convert convolutionary signal to additive form [20]. This technique is widely used to extract power spectrum from non-homogenous materials where intensity variation is substantial. The flow chart of the process is depicted in Figure-3 and the output of each step is shown in Figure-4. The first stage of the process is to transform the filtered signal (Figure-4a) via Fourier transformation to a power spectrum (Figure-4b). Then with logarithmic operation, the multiplicative relationship between mean echo wavelet and the grain impulse response is converted to additional operation in the frequency domain (Figure-4c). Grain signal power cepstrum is subsequently obtained by taking the inverse Fourier transform of the power spectrum (Figure-4d). Short-pass lifter [5] is employed to minimize the effect of random pattern of the grain echoes such that the possibility of wavelet recovery is improved. By taking the Fourier transform of the wavelet magnitude cepstrum, we have logarithm of wavelet magnitude spectrum from which absolute magnitude spectrum is obtained (Figure-4e). The wavelet magnitude spectrum gives information about the center frequency and bandwidth of the signal.

The accuracy of the homomorphic process was established by comparing the magnitude spectral of a distinct backscattered echo obtained via FFT and homomorphic process. Results obtained (Figures 4f and g) indicated equal center frequency (2.7344 MHz) with 3.27% higher value of bandwidth for homomorphic process. The slightly higher bandwidth is attributable to the complex nature of the signal processing technique. The centre frequency was used to establish frequency shift and attenuation of the samples.

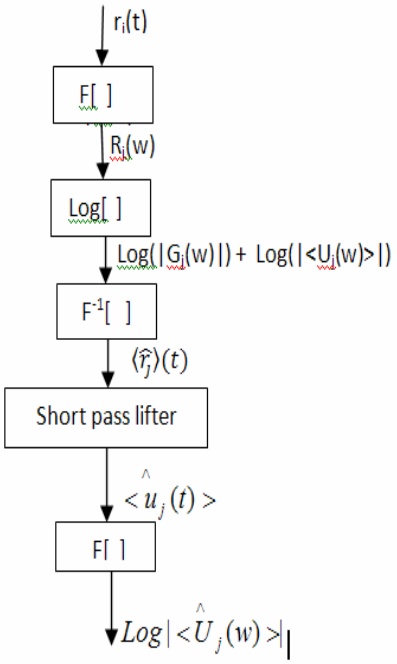

Figure-3. Flow chart for the homomorphic signal processing.

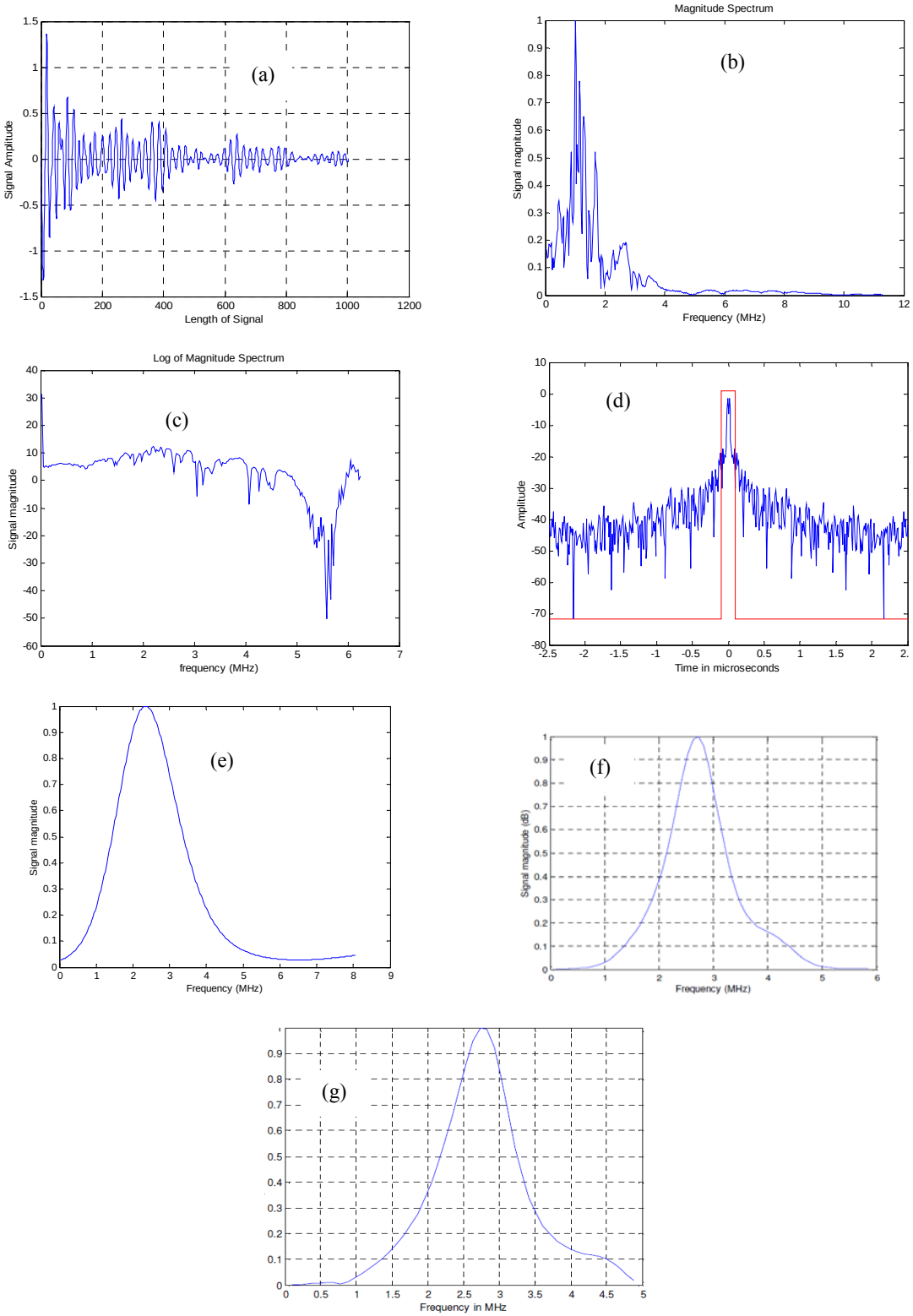

Figure-4. Stages in homomorphic signal processing (a) de-noised signal (b) power spectrum (c) logarithm of power spectrum (d) inverse FT of (c) showing rectangular window (e) wavelet magnitude spectrum. Comparison of power spectrum for the reference steel using (f) homomorphic process (g) FFT. The grids serve as guides for the eyes.

4. RESULTS AND DISCUSSIONS

In this session, I discussed the procedure for the determination of optimal window length as well as the results of the time domain and homomorphic analyses.

4.1 Determination of optimal window length

Window length (length of the rectangular filter) refers to the number of data point covered by rectangular window on which the wavelet recovery process significantly depends on. If the window length is too large, spurious pattern of the recovery wavelet is observed (Figures 5a, b and c) while a narrow window truncates some necessary information for wavelet recovery (Figures 5e and f). Figure-5d shows a magnitude spectrum with Gaussian shape and positive skewness with neither a spurious pattern nor truncation of information in comparison with others. In addition, analysis of the change in the bandwidth reveals an increase of 179% as the window length is reduced from 6 to 2 with a corresponding increase of 33% of the center frequency. Rectangular window of length 6 produced the best wavelet spectrum and was chosen as the optimal window length and subsequently adopted for further homomorphic process.

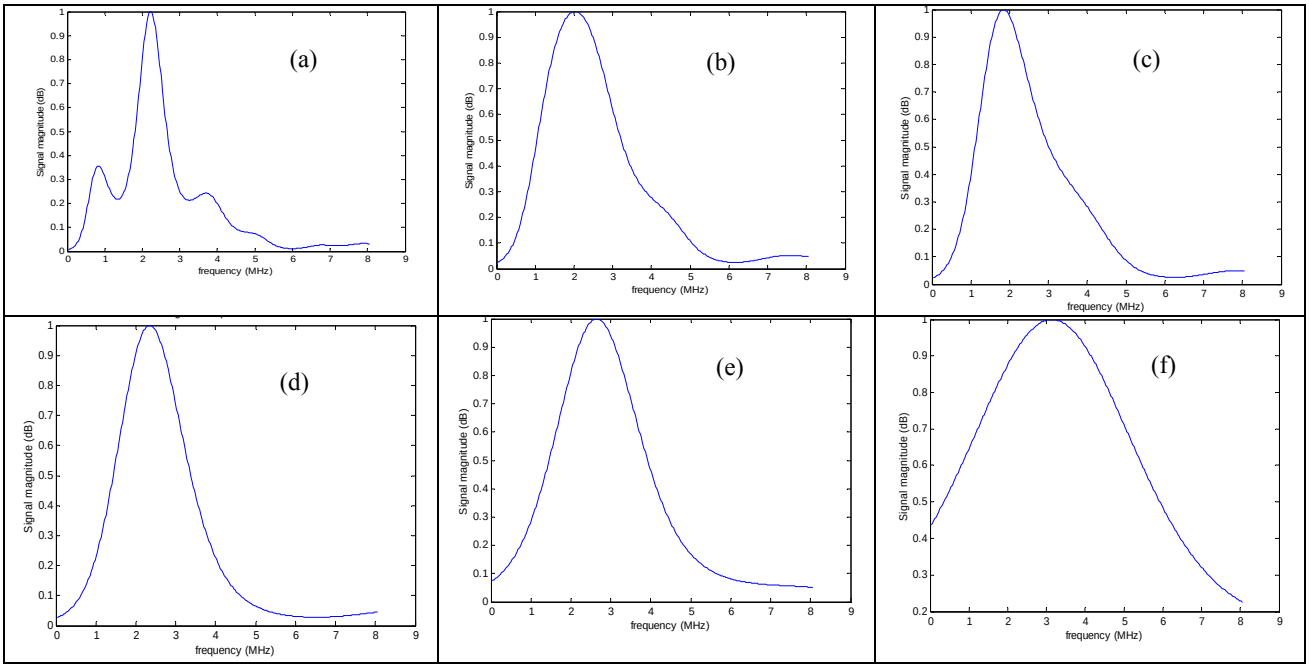

Figure-5. Wavelet magnitude spectrum for a window length of (a) 20 (b) 12 (c) 8 (d) 6 (e) 4 (f) 2. The frequency domain based homomorphic process allows the monitoring of the center frequency of the magnitude spectrum in comparison to the center frequency of the exciting transducer.

4.2 Time domain analysis

Histogram of the signal amplitudes is a practical way of evaluating the backscattered grain signal and comparative study of the attenuation property of each material. Figure-6 shows three histograms, each randomly selected from 49 histograms of the signals obtained from each sample. These histograms show that there is relative change between the two regions of the signals due to changes in the absorption and scattering characteristics of the samples. Histograms of region j+1 display a shift toward lower amplitude compared to histograms of region j. In addition, the histograms indicate differences in the shift rates. EGRG exhibits higher frequency shift compared to GRG and then compared to CB. Regions j+1 shift more significantly towards the lower amplitudes.

Statistical analysis of the histograms (Table-1) shows that scattering and attenuation are higher in EGRG (38.7%) compared to GRG (36.51%) and CB (27.66%) adjudged by the changes in the mean amplitudes. The standard deviation indicates uniformity in attenuation and scattering from region j to region j+1 and it shows that scattering and attenuation are more uniform in GRG considering the standard deviation of the two regions, which are smaller than those of CB and GRG. However, all the data indicate that attenuation is high in all samples. The skewness of the data proves that all the samples are asymmetrically distributed from negatively skewed region j to positively skewed region j+1 and the shift in values of skewness increases from EGRG to CB confirming the earlier explanation about material uniformity in the distribution of the scatterers.

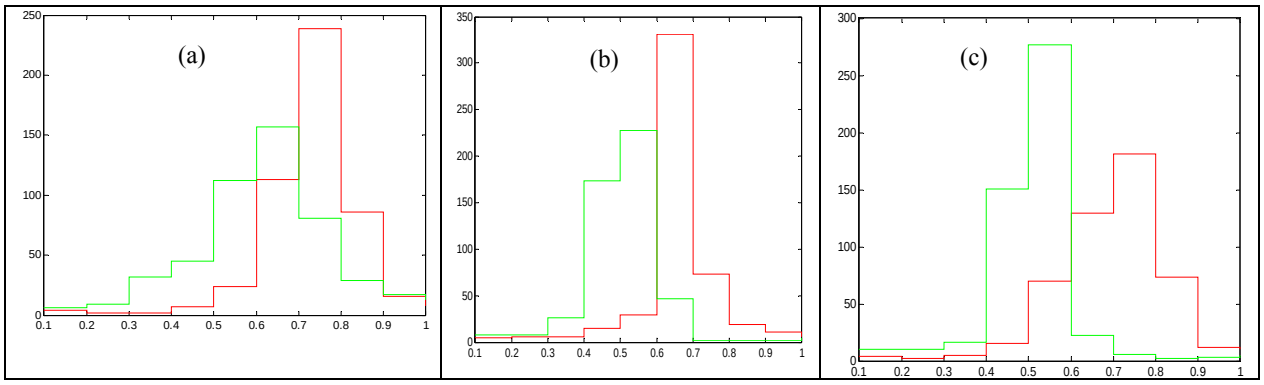

Figure-6. Typical histograms obtained from (a) CB (b) GRG (c) EGRG. Red and green colours indicate region j and j+1 respectively. The vertical axis contains the signal amplitude.

Table-1. The properties of the signals from the three samples. 'std' denotes standard deviation, j indicates region j and j+1 denotes region j+1.

Parameter	CB			GRG			EGRG		
	j	j+1	% shift	j	j+1	% shift	j	j+1	% shift
Mean	0.0047	0.0034	27.66	0.0063	0.0040	36.51	0.0070	0.0043	38.57
Std.	0.3507	0.0655	81.32	0.2530	0.0673	86.40	0.2439	0.0083	96.60
Skewness	-0.2861	0.0145	105.06	-1.044	0.3561	134.12	-1.827	0.0318	101.17

4.3 Center frequency shifts and attenuation

The shifts in the center frequencies due to ultrasonic wave attenuation for some selected grids as obtained through homomorphic process for all the samples are shown in Table-2. These values confirm that all the samples exhibit attenuation and that the attenuations vary from point to point within each sample and significantly across the three samples as noted by the percentage frequency shifts. CB is observed to have the lowest frequency shifts while highest frequency shift is obtained for EGRG. The difference in the frequency shifts is attributed to the changes in the scattering and absorption rate within the samples continuum. Across the samples, a downward shift in frequency is noted in comparison with the center frequency of the reference steel sample with known microstructure uniformity. The statistical summary of the center frequencies properties are shown in Table-2 (d). The statistical analysis shows that CB has the highest centre frequency (μ = 2.3891MHz and σ = 0.0239MHz) followed by GRG (μ = 2.2695MHz and σ = 0.0254MHz) and then EGRG (μ = 2.2102MHz and σ = 0.0264MHz). This cross analysis justified by the differences in standard deviations connotes that the scatterers within cement board are smaller and more uniform compared to others. EGRG is observed to have largest size of scatterers and attenuators. This confirms that the size of attenuators in EGRG is of highest value.

As earlier stated, EGRG is a mixture of GRG and polymer, thus the added polymer increases the reinforcement via addition of more scatterers. In other words, the higher the fraction of the reinforcement (like glass fiber, polymer) in the mixture, the more the number of scatterers that are likely to be present within the material structure. These scatterers, though responsible for improving some physical properties like strength and other mechanical properties, confer lower acoustic characteristics on the material and ultrasonic waves are greatly scattered and attenuated.

Numerical estimation of the attenuation coefficients was determined using equation (9) and shown in Figure-7. Each curve is obtained from a typical grid within the materials. The frequency range over which results of the analysis was coherent is justified by the bandwidth of the transducer (2.0286-3.4402 MHz) which has a great influence on the values obtained at various frequencies. Beyond the upper boundary, random, incoherence and unreliable attenuation coefficients are obtained (not shown in Figure-7). In addition, attenuation coefficients show non-coherence and unrealistic relationship where magnitude spectra of region j+1 became higher than those of region j. CB is observed to have the lowest attenuation coefficient followed by GRG while highest values of the attenuation coefficients are obtained for EGRG within the range of the transducer bandwidth. Both GRG and EGRG exhibit close frequency dependent attenuation behaviour confirming the earlier observation that they have closely related microstructural distribution. However, CB displays a clearer dependency on frequency. This Figure obviously supports the previous results of both time domain analysis and homomorphic processing. Thus the result clearly demonstrates the application of homomorphic analysis for determination of frequency shifts and ultimately for material characterization. Though, both time-domain and

homomorphic analyses are effective for characterizing materials, however, homomorphic process gives a quantitative comparison and thus performs better than time domain analysis.

To ensure that the experimental process is repeatable, six measurement repetitions were made on cement board using some randomly selected grid. The results of grid 14 indicate a mean value of 2.5079 MHz and standard deviation of 0.0105 MHz. The negligible value of the standard deviation shows that the center frequencies are significantly equal. Comparison of the mean value with the value obtained previously (2.5146 MHz) shows a difference of 0.26%. In addition, grids 10, 22, 45 were selected in random and tested in 10 repetitions each. The results were 2.6690, 2.6588 and 2.6635MHz for the average values of the center frequencies and 0.0160, 0.0143 and 0.0191 for standard deviations. These results show that, though center frequencies are affected by repetition (due to variation in the amount of couplant and pressure applied during sample scanning), the effect is insignificant and can be incorporated within an acceptable experimental limit. Therefore, if the signals were carefully obtained, the effect of repetition is virtually insignificant and thus the shifts in the frequencies obtained can be confidently attributed to the scatterers within the samples rather than artifacts of signal acquisition and processing.

Table-2. Typical frequencies shifts for (a) CB (b) GRG and (c) EGRG. Summary of signal properties is indicated in (d)

(a)

Grid	14	25	27	31	36	43	47	51	57	75
Region j	2.368	2.5634	2.441	2.075	2.271	2.417	2.441	2.2945	2.295	2.295
Region j+1	2.246	2.2705	2.271	2.051	2.099	2.246	2.344	2.271	2.271	2.271
% shift	5.155	11.4286	7.000	1.177	7.527	7.071	4.000	1.064	1.064	1.064

(b)

Grid	14	25	27	31	36	43	47	51	57	75
Region j	1.977	1.953	1.904	2.002	2.246	2.295	1.978	1.953	1.929	2.124
Region j+1	1.855	1.856	1.807	1.953	1.879	2.026	1.879	1.929	1.929	1.879
% shift	6.172	5.000	5.128	2.500	16.304	11.702	4.938	1.250	0.000	11.494

(c)

Grid	14	25	27	31	36	43	47	51	57	75
Region j	2.343	2.0020	2.099	2.026	1.977	2.026	2.002	2.075	1.879	1.953
Region j+1	2.002	1.977	1.855	1.684	1.928	1.660	1.587	1.758	1.856	1.611
% shift	17.073	1.219	11.627	16.867	2.469	18.072	20.732	15.294	1.299	17.500

d)

Statistical Parameters	Reference data	CB	GRG	EGRG
Mean center frequency (MHz)	2.5635	2.3891	2.2695	2.2102
Mean bandwidth (MHz)	1.4689	1.3259	1.4138	1.3325
Standard deviation	-	0.0239	0.0254	0.0094
Skewness	-	0.1343	0.5616	1.1025

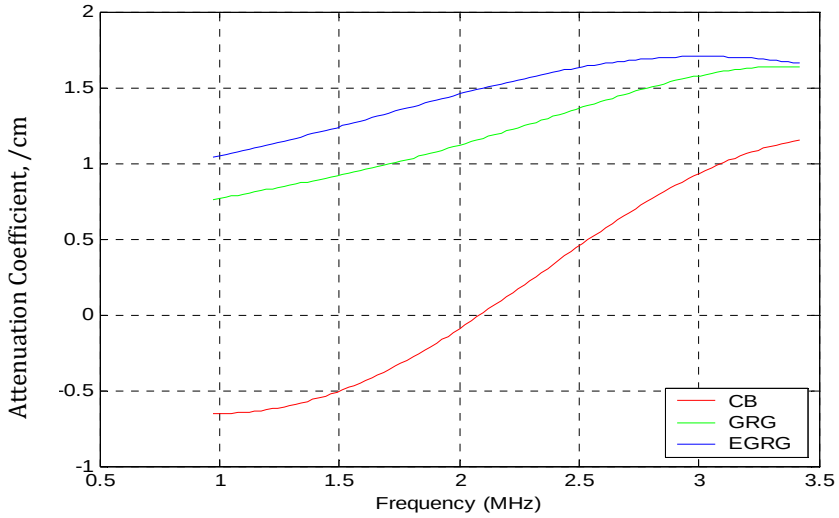

Figuire-7. Frequency dependent attenuation coefficients for the samples under study.

5. CONCLUSIONS

Time domain and homomorphic signal analysis have been proved to be suitable for extraction of wavelet magnitude spectral of gypsum based material using an optimized window length. Accuracy of homomorphic process was established by comparing the magnitude spectral of a distinct backscattered echo obtained via FFT and that of homomorphic process using steel reference sample. Results obtained indicated equal center frequencies (2.7344 MHz) with 3.27% higher value of bandwidth for homomorphic process. Comparative study of histograms between segmented regions within the samples' signals clearly indicated a continuous change in the attenuation. Time domain analysis confirmed increase in the attenuation from cement board to exterior glass fiber reinforced gypsum. The percentage shifts in statistical parameters have been consistent as well. The experimental results show downward shift in the center frequencies compared to that of reference steel sample. Graph of frequency dependent attenuation coefficient also confirmed differences in attenuation rate among the three materials. Cement board is observed to have lowest attenuation coefficient followed by GRG while EGRG has the highest value within the transducer bandwidth. Attenuation increases with increase in frequency within the transducer bandwidth (2.0286-3.4402 MHz) for all the three materials. Tests of repetitions confirm that the observed frequency changes are due to sample non-uniformity and not signal processing artifacts.

REFERENCES

[1] Asafa T. B. 2008. Ultrasonic evaluation of plaster boards. London: Unpublished M.Sc Thesis of University College London, U.K.

[2] Aggelis D. 2011. Advanced Ultrasonic Characterization of Fresh Cementitous Materials. Nova Science Publishers.

[3] Papadakis E P. 1965. Ultrasonic attenuation caused by scattering in polycrystalline metals. The journal of Acoustic Society of America. 37(4).

[4] Evans A G., Kino G S., Khuri-Yakub B T. and Tittmann B R. 1977. Destructive testing. 35(4): 85-96.

[5] Saniie J., Wang T. and Bilgutay N M. 1989. Analysis of homomorphic processing for ultrasonic grain characterization. IEE transaction on ultrasonics, ferroelectrics and frequency control. 34(3): 365-375.

[6] Saniie J. and Bilgutay N M. 1986. Qualitative grain size evaluation using ultrasonic backscattered echoes. Journal of Acoustic Society of America. 80(6): 1816-1824.

[7] Fukuhara M., Zhang W., Louzguine-Luzgin D V and Inoue A. 2007. Ultrasonic attenuation properties of glassy alloys in views of complex viscoelasticity. Applied Physics Letter. 90(131902).

[8] Cantrell J. and Yost W. 2001. Nonlinear ultrasonic characterization of fatigue microstructures. International Journal of Fatigue. 23 , S487-S490.

[9] Bouda A. L. 2003. Grain size influence on ultrasonic velocities and attenuation. NDT and E International. 36 (1-5).

[10] Djordjevic B. 2009. Ultrasonic chracterization of advanced composite materials. The 10th International Conference of the Slovenian Society for Non-Destructive Testing: Application of Contemporary Non-Destructive Testing in Engineering. pp. 47-57. Ljubljana, Slovenia: The Slovenian Society for Non-Destructive Testing.

[11] Tasker C G., Milne J M. and Smith R L. 1990. Recent work at the National NDT Centre on concrete inspection. British Journal of NDT. 32(7): 355-359.

[12] Gaydecki P A., Burdekin F M., Damaj W., Johns D G. and Payne P. 1992. The propagation and attenuation of medium-frequency ultrasonic waves in concrete: A signal analytical approach. Measurement Science and Technology. 3(1): 126-134.

[13] Landis E N. and Shah S P. 1995. Frequency-dependent stress wave attenuation in cement-based materials. J. Engrg. Mech., ASCE. 121(6): 737-743.

[14] Joseph O. O. and Laurence J J. 1999. Attenuation measurements in cement-based materials using laser ultrasonics. Journal of Engrg. Mech. 125(6): 637-647.

[15] Laurence J J. and Joseph O. O. 2000. Effects of aggregate size on attenuation of Rayleigh surface waves in cement-based materials. Journal of Engrg. Mech. 126(11): 1124-1130.

[16] Botvina L R., Franklin L J. and Bridge B. 2000. A new method for accessing the mean grain size of polycrystalline materials using ultrasonic NDE. Journal of Material Sciences. 35: 4673-4683.

[17] Bray D E. and McBride D. 1992. Nondestructive testing techniques 1st Ed. New York: John Wiley and Sons, Inc. ISBN 0-471-52513-8. pp. 253-320.

[18] Sarpun I H., Özkan V., Tuncel S. and Ünal R. 2007. Determination of mean grain size by ultrasonic methods of tungsten carbide and boron carbide composites sintered at various temperatures. 4th International Conference on NDT. Chania, Crete-Greece.

[19] Hirsekorn S. 1982. The scattering of ultrasonic waves by polycrystal. Journal of Acoustic Society of America. 72(3): 1021-1031.

[20] Shull P J. 2002. Non-destructive evaluation. 1st Ed. New York: Marcel Dekker Inc. ISBN 0-8247-8872-4. pp. 105-120.

[21] Kelly S P., Farlow R. and Hatward G. 1996. Application of through-Air Ultrasound for Rapid NDE scanning in the aerospace industry. IEE Transaction on Ultrasonic, Ferroelectrics and Frequency Control. 43(4): 581-591.